Ultra-Low Phase Noise Crystal Oscillators

Jeremy Everard
Department of Electronics,
University of York,
Heslington, York, YO10 5DD, UK
jkae@ohm.york.ac.uk

Keng Ng
Formerly Department of Electronics
University of York
Heslington, York, YO10 5DD, UK

***Abstract*— This paper describes, in general terms, the theory and design of ultra-low noise crystal oscillators based on SC cut crystal resonators operating at 10MHz. These oscillators demonstrate -118dBc/Hz at 1Hz and -147dBc/Hz at 10Hz offsets. The noise floor was <-160dBc/Hz. To achieve this performance a feedback oscillator has been designed by optimizing the individual elements separately and then combining them to form the final oscillator. The parameters for the resonators, tuning networks, phase shifters and amplifiers were optimized both theoretically and experimentally.**

I. INTRODUCTION

The oscillator in communication and measurement systems, defines the reference signal onto which modulation is coded and later demodulated. The flicker and phase noise in such oscillators are central in setting the ultimate performance limits of modern communications, radar and timing systems. These oscillators are therefore required to be of the highest quality for the particular application.

Crystal oscillators offer a universal solution due to the precise resonant frequency, very high Q and controllable temperature coefficients.

II. PHASE NOISE THEORY

It is important to develop a simple model to calculate and predict the noise performance of an oscillator. Leeson [1] demonstrated an equation which gives useful information about the phase noise but the optimum conditions for minimum noise are not clear. Parker [2] demonstrated an optimum condition for a modified version of Leeson's equation. It is useful, however, to develop a simple model, from first principles, which enables an accurate and clearly understood equation to be derived.

A suitable model is shown in figure 1 [3][4]. This consists of an amplifier with two inputs which are added together. These represent the same input but are separated to enable one to be used to model the noise input and the other for feedback. The resonator is represented as an LCR circuit where any impedance transformation is achieved by varying the component values. This circuit, through positive feedback, operates as a Q multiplication filter but also contains the additional constraint that the AM noise is suppressed in the limiting process. This causes the upper and lower sidebands to become coherent and has been defined as conformability by Robbins [5]. The model is put in this form to highlight all the effects, which are often not clear in a block diagram model.

A general equation for the phase noise can be derived as shown in equation 1 [3] which incorporates a number of operating conditions including power and the output and input impedances. F is the operating noise factor which includes the amplifier parameters under the oscillating operating conditions, k is the Boltzmann constant and T is the operating temperature. Q_0 is the unloaded Q, Q_L is the loaded Q, f_0 is the oscillator frequency and Δf is the offset frequency. P is the power in the oscillator which can be defined in two ways. P_{AVO} is the power available from the output of the amplifier and P_{RF} is the total power dissipated in the input, output, and equivalent loss resistances. N and A are integer variables which can be 1 or 2 dependent on the definition of P.

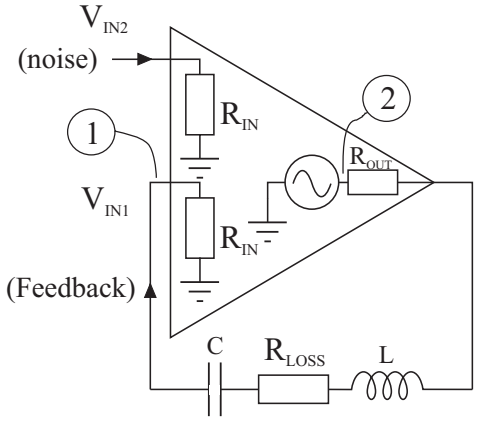

Figure 1 Oscillator Model

$$L(f) = A.\frac{FkT}{8(Q_0)^2(Q_L/Q_0)^2(1-Q_L/Q_0)^N P}\left(\frac{f_0}{\Delta f}\right)^2 \quad (1)$$

where:

1. $N = 1$ and $A = 1$ if P is defined as P_{RF} and R_{OUT} = zero.
2. $N = 1$ and $A = 2$ if P is defined as P_{RF} and $R_{OUT} = R_{IN}$.
3. $N = 2$ and $A = 1$ if P is defined as P_{AVO} and $R_{OUT} = R_{IN}$.

If we take expansion 3 and show the full equation including the impedances, we obtain equation 2 [3].

$$L(f) = \frac{FkT}{32Q_0^2(Q_L/Q_0)^2(1-Q_L/Q_0)^2 P_{AVO}} \left(\frac{(R_{OUT}+R_{IN})^2}{R_{OUT}.R_{IN}}\right)\left(\frac{f_0}{\Delta f}\right)^2 \quad (2)$$

The bracket including R_{OUT} and R_{IN} is minimum when $R_{OUT} = R_{IN}$ causing the whole bracket to equal 4. Equation 2 then simplifies to equation 3:

$$L(f) = \frac{FkT}{8Q_0^2\left(\frac{Q_L}{Q_0}\right)^2\left(1-\frac{Q_L}{Q_0}\right)^2 P_{avo}}\left(\frac{f_0}{\Delta f}\right)^2 \quad (3)$$

This equation will be used in the analysis for the noise performance and gain requirements.

This equation has a further minimum when Q_L/Q_0 = ½ and hence when the insertion loss of the resonator is 0.25 (–6dB). This minimum occurs because the amplifier gain is set by the insertion loss of the resonator which is:

$$S_{21} = (1 = Q_L/Q_0) \quad (4)$$

This was first described by Parker in [2].

Under optimum conditions:

$$L(f) = \frac{2FkT}{Q_0^2 P_{AVO}}\left(\frac{f_0}{\Delta f}\right)^2 \quad (5)$$

Equation (5) is similar to Leeson's equation [1], although Leeson's equation used the loaded Q, Q_L, and the power incident on the input, P_I. Taking Leeson's Equation from [1] where the flicker noise parameters and the noise floor are left out, we obtain:

$$S_\phi(f) = \frac{FkT}{2Q_L^2 P_I}\left(\frac{f_0}{f}\right)^2 \quad (6)$$

where $S_\phi(f)$ is the spectral power density of phase fluctuations in radians squared per Hertz.

Taking the conditions that $P_I = P_{AVO}/4$ and $Q_L = Q_0/2$, based on the optima derived from equation (3), and assuming small angle modulation, then Leeson's equation becomes:

$$L(f) = \frac{S_\phi(f)}{2} = \frac{4FkT}{Q_0^2 P_{AVO}}\left(\frac{f_0}{f}\right)^2 \quad (7)$$

This version of Leeson's equation has the same form as equation (3) but is twice it's value. This is because equation (3) incorporates the assumption that limiting causes the phase noise component to be half the total thermal noise. This lower noise floor is confirmed in [6] where they have shown 'theoretically and experimentally that the single sideband PM (and AM) noise floor due to thermal noise' (at room temperature) 'is -177dBc/Hz relative to a carrier input power of 0dBm'.

It should be noted that the noise factor, F, was assumed to be constant in this optimization. The noise factor may however vary with source impedance and hence Q_L/Q_0 as described in [7]. The noise factor may also show a power dependence which can be affected by both the device type and the amplifier topology. Examples of the effects of gain compression on the thermal (additive noise) and transposed flicker noise (modulation noise) are shown in [7]. If the inter-dependence is known then this can be incorporated to modify the optimum value of Q_L/Q_0.

Based on equation 1, plots of noise degradation with Q_L/Q_0 are shown in Figure 2. This shows the phase noise degradation for the two different definitions of power (P_{AVO} or P_{RF}). Also included are measurements on an oscillator in which the amplifier had a very low output impedance. [4]

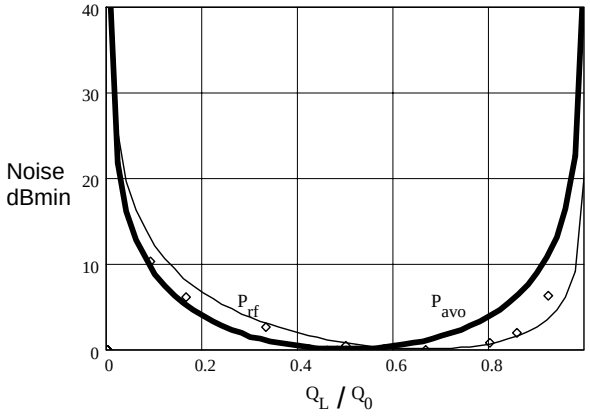

Figure 2 Phase Noise, dBmin vs Q_L/Q_0

To obtain further insight, a plot of noise degradation with resonator insertion loss and hence closed loop gain is shown in Figure 3. This gives a more obvious indication of the allowable tolerances on the insertion loss of a resonator. It can be seen that only one dB of noise degradation occurs when the insertion loss is within the bounds of 3.5 to 9.5dB.

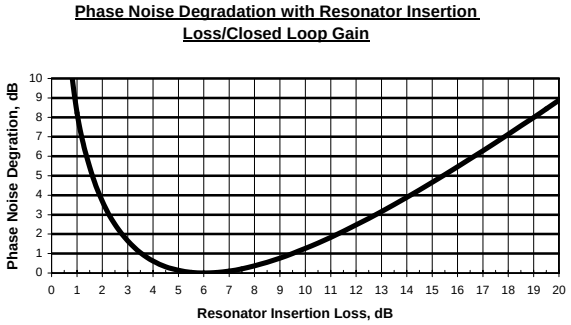

Figure 3, Phase noise degradation with resonator insertion loss/open loop gain

It should be noted that the optima, just discussed, apply if the noise is thermal (additive) noise and also only apply to the skirts of the phase noise. For far out noise to be minimum the gain should be kept low (Q_L/Q_0 low) and for reduced transposed flicker noise the loaded Q should be higher. However it is a good starting point.

The equation used to calculate the phase noise, used in the simulations and measurements shown later, is shown below in equation 8. The right hand term is based on equation 3, the middle term shows noise outside the resonator bandwidth (far from carrier noise) and both these terms are multiplied by a flicker noise component ($1 + F_C/f$). The left hand term includes the buffer amplifier after the output coupler and is still assumed to be limited by the phase noise measurement (therefore 2P). The '1' refers to the phase noise of a single oscillator. This is changed to 2 when the combined noise of two identical oscillators is being displayed.

$$L(f)=10\mathrm{Log}\left[1\left[\frac{F_2kT}{C_0 2P}+\left(1+\frac{Fc}{f}\right)\left(\frac{F_1kT}{2P}\left(\frac{1}{\left(1-\frac{Q_L}{Q_0}\right)}\right)+\frac{F_1kT}{8(Q_0)^2\left(\frac{Q_L}{Q_0}\right)^2\left(1-\frac{Q_L}{Q_0}\right)^2 P}\left(\frac{f_0}{f}\right)^2\right)\right]\right] \quad (8)$$

III. OSCILLATOR CONFIGURATION

The feedback oscillator configuration is shown in Figure 4. This consists of: an amplifier and output coupler; a fixed phase shifter to obtain the correct open loop phase shift; a voltage controlled phase shifter to provide narrow band tuning with negligible noise degradation; a spur rejection filter; and the crystal resonator. Each element was designed and optimized separately.

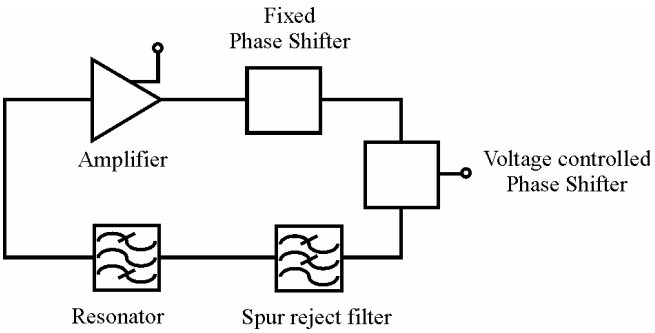

Figure 4, Feedback Oscillator Configuration

A. *AMPLIFIERS*

The amplifiers should offer:

1. Well defined input and output impedance
2. Low noise figure
3. Low Residual Flicker Noise using optimum bias
4. Low dependence on power supply noise and low regulator noise
5. Well defined limited output power
6. Smooth monotonic saturation characteristics with negligible change in parameters
7. Unconditional stability both in the linear and saturation regions

All of these parameters are interdependent and therefore need to be optimised carefully.

B. *The Crystal Resonator*

The crystals used were Nofech 10MHz SC cut resonators. The manufacturers parameters were approximately: RR ~ 53Ω, Q_0 ~ 1.3M and turnover temperature, TO, ~ 82ºC.

A simple model for the crystal (Fig 5) was developed based on S parameter measurements. The crystal was placed in a metal jig on a 50Ω microstrip transmission line and the series, parallel and first spur frequencies were measured (Fig 6). The loaded Qs and insertion loss were also measured. The loaded Q of the series resonance was 500,000 (BW = 20Hz) with an insertion loss of 3.47dB. Note care should be taken to ensure that the sweep rate is sufficiently low to obtain accurate results. It is also quite easy to see ringing on the network analyzer if the sweep is too fast.

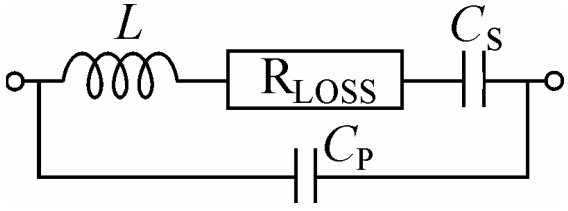

Figure 5, Model for crystal resonator

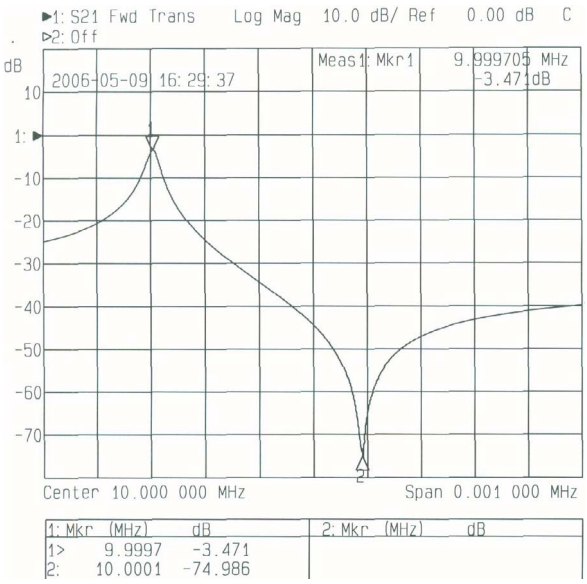

Figure 6, S_{21} for Crystal Resonator

Simplifying the model to just the series resonant elements, it is possible to use the equation $S_{21} = (1 - Q_L/Q_0)$ to estimate the unloaded Q. From this equation $Q_0 = 1.52M$ (which is a little high and higher than the manufacturers parameters). Note that more accurate modeling can be achieved by including further components in this model. By using the ratio of the series and parallel resonances the other components can be calculated using:

$$\frac{f_P}{f_S} = \sqrt{1 + \frac{C_S}{C_S + C_P}} \qquad (9)$$

C. *Spurious rejection filter*

A spurious response occurs in these crystals at 10.88 MHz (with very similar parameters to the wanted resonance [8]) and a filter with negligible loss at the wanted resonance was incorporated into the whole circuit.

D. *TUNING ELEMENTS*

Frequency tuning is typically achieved by incorporating the varactor diodes either into the resonator or by using phase shift tuning separate from the resonator as illustrated in Figure 4. Phase shift tuning has the advantage that it does not degrade the resonator unloaded Q and the phase noise degradation can be accurately calculated. This group has shown (theoretically and experimentally) that the noise performance degrades with a $\cos^4\theta$ relationship [3] [7]. Therefore an open loop phase error of 45º causes 6dB degradation + the insertion loss of the phase shifter. This is illustrated in figure 7.

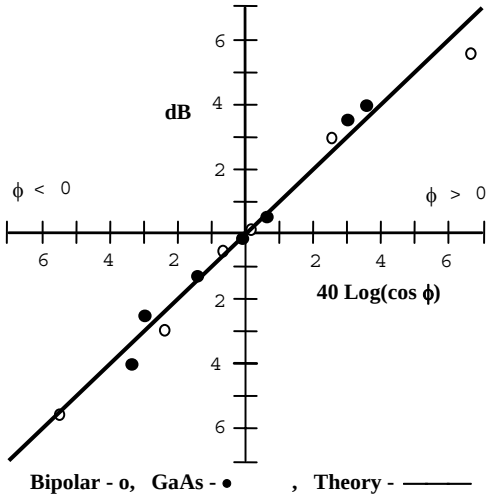

Figure 7 Phase noise degradation with open loop phase error

The phase shifter should have low insertion loss and a linear phase vs frequency response. A voltage controlled phase shifter was therefore designed and the amplitude and phase response are shown in Figure 8

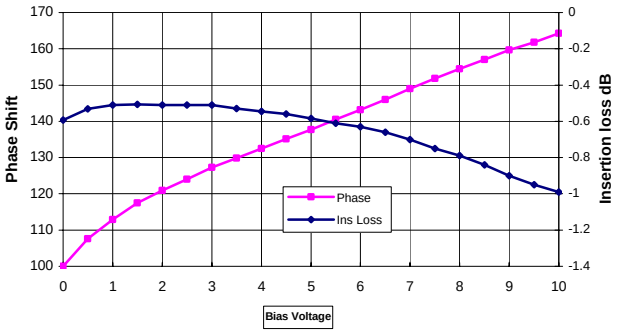

Figure 8, Insertion loss and phase shift vs voltage

IV. OSCILLATORS AND NOISE MEASUREMENTS

The components were connected as a feedback oscillator with a further phase shift element incorporated to ensure that the open loop phase error was zero or N x 360 as shown in Figure 4.

The phase noise was measured using the experimental setup shown in figure 9. Two oscillators were connected to an HP 3048 phase noise measurement system via 20dB Minicircuits buffer amplifiers and 3 and 10dB attenuators respectively. Both oscillators were operated using batteries with an internal battery used for varactor bias on one of the oscillators. The oscillators and resonators were operated at room temperature. No indication of injection locking was observed.

Three measurements were made. The first two measurements use an amplifier with 50Ω I/P and O/P impedances but with a high noise figure of 7.5dB and with a

power in the crystal of 100µW and 200µW. The third measurement used the amplifier now with noise matching to achieve a noise figure of 1.8dB and a power in the crystal of 200µW

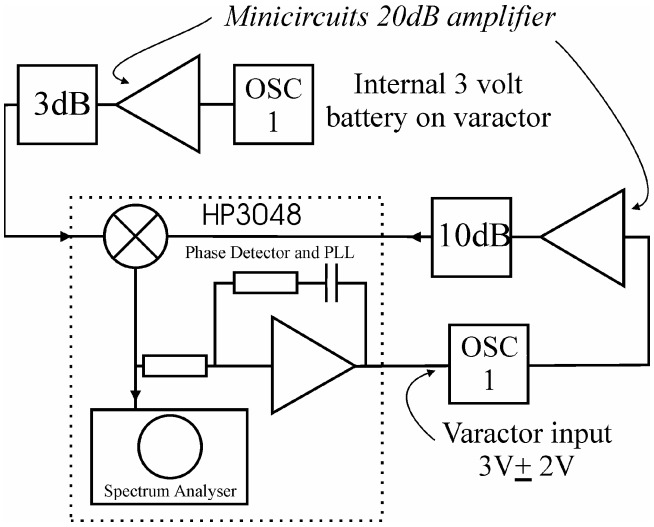

Figure 9, Phase Noise Measurement System

A. *Results from Measurements One and Two*

The results for the first two measurements are shown in Figure 10. The upper curve is for 100µW and the lower curve is 200µW respectively. To obtain the curve fit for the lower curve a flicker noise corner of 80Hz was used.

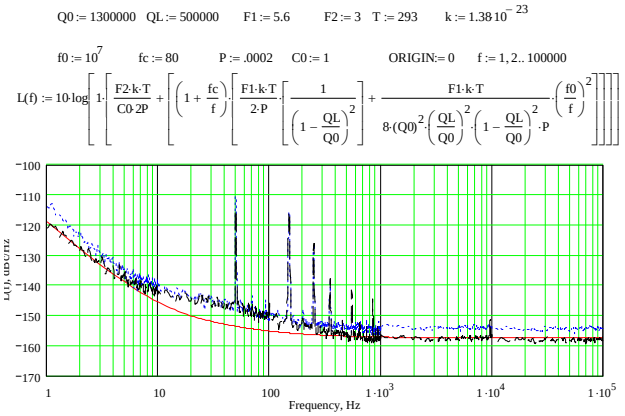

Figure 10. Phase Noise plots using

B. *Results from Measurement Three*

The noise figure of the amplifier was optimized for a lower noise figure of 1.8dB and the power in the crystal resonator was maintained at 200µW. The buffer amplifiers were also operated from batteries for this measurement which is why the spurs are reduced. It is also possible that this has reduced the phase noise from 10 to 500Hz. The third measurement is shown in Figure 11. To obtain a curve fit the flicker noise corner was set to 300Hz. It is interesting to note that measurement 3 is better than measurement 2 by about 5dB (difference in noise figures) for most of the offset range except for very close to carrier (1 – 5Hz) and for the hump from 10 to 200Hz in measurement 2. This will be further investigated.

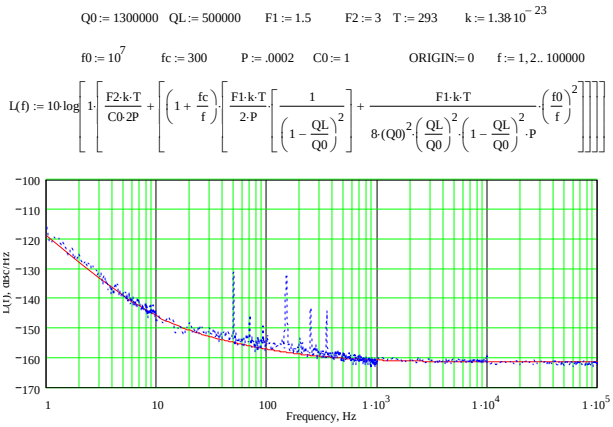

Figure 11, Phase Noise plot with low noise figure amplifier and crystal power of 200µW

V. Conclusions

Very low noise crystal oscillators operating at 10MHz have been built. The best performance demonstrated was -118dBc/Hz at 1Hz offset and -147dBc/Hz at 10Hz offset. The noise floor was less than -160dBc/Hz.

VI. References

[1] D.B. Leeson, A Simple Model of Feedback Oscillator Noise Spectrum", Proceedings of the IEEE, 54, pp. 329-330, Feb. 1966.

[2] T.E. Parker, "Current Developments in SAW Oscillator Stability", Proceedings of the 31st Annual Symposium on Frequency Control, Atlantic City, New Jersey, 1977, pp. 359–364.

[3] Jeremy Everard, "Fundamentals of RF Circuit Design with Low Noise Oscillators", ISBN: 0-471-49793-2, Wiley, Dec. 2000 reprinted Oct. 2002.

[4] Jeremy Everard, "Low Noise Power Efficient Oscillators: Theory and Design," Proceeding of the IEE, pt G, 133, No.4, pp172-180, 1986.

[5] W.P. Robins, "Phase Noise in Signal Sources," IEE, Peter Perigrinus, 1992.

[6] A. Hati, D. A. Howe, F. L.Walls, and D.Walker, "Noise figure vs PM noise measurements: A study at microwave frequencies," Proc. IEEE Int. Freq. Contr. Symp. Digest, 2003, pp. 516–520.

[7] K.K.M. Cheng and J.K.A. Everard, "Noise Performance Degradation in Feedback Oscillators with non zero Phase Error". Microwave and Optical Technology Letters, 4, No. 2, pp. 64 - 66, 1991.

[8] J. Vig, "Quartz Crystal Resonators and Oscillators For Frequency Control and Timing Applications - A Tutorial," January 2007. http://www.ieee-uffc.org/freqcontrol/tutorials/vig3/vig3.ppt